Journal of Power Sources 195 (2010) 6496–6499

Contents lists available at ScienceDirect

Journal of Power Sources

journal homepage: www.elsevier.com/locate/jpowsour

Short communication

Improved performance of Pd electrocatalyst supported on three-dimensional nickel foam for direct ethanol fuel cells

You-Ling Wang[a], Yong-Qing Zhao[a], Cai-Ling Xu[a,*], Dan-Dan Zhao[a], Mao-Wen Xu[b], Zhong-Xing Su[a], Hu-Lin Li[a]

[a] Key Laboratory of Nonferrous Metal Chemistry and Resources Utilization of Gansu Province, School of Chemistry and Chemical Engineering, Lanzhou University, Lanzhou 730000, China
[b] College of Chemistry and Chemical Engineering, Xinjiang Normal University, Urumqi 830054, China

ARTICLE INFO

Article history:
Received 10 March 2010
Received in revised form 8 April 2010
Accepted 8 April 2010
Available online 14 April 2010

Keywords:
Palladium electrocatalyst
Nickle foam
Hierarchical structure
Ethanol oxidation

ABSTRACT

To improve the performance of direct ethanol fuel cells (DEFCs), a three-dimensional (3D), hierarchically structured Pd electrode has been successfully fabricated by directly electrodepositing Pd nanoparticles on the nickel foam (referred as Pd/Nickel foam electrode hereinafter). The electrochemical properties of the as-prepared electrode for ethanol oxidation have been investigated by cyclic voltammetry (CV). The results show that the oxidation peak current density of the Pd/Nickel foam electrode is 107.7 mA cm^{-2}, above 8 times than that of Pd film electrode at the same Pd loading (0.11 mg cm^{-2}), and a 90 mV negative shift of the onset potential is found on the Pd/Nickel foam electrode compared with the Pd film electrode. Furthermore, the peak current density of the 500th cycle remains 98.1% of the maximum value for the Pd/Nickel foam electrode after a 500-cycle test, whereas it is only 14.2% for the Pd film. The improved electrocatalytic activity and excellent stability of the Pd/Nickel foam electrode make it a favorable platform for direct ethanol fuel cell applications.

1. Introduction

Recently, DEFCs have aroused much attention due to the advantages of ethanol over other fuels, such as high energy density, easy storage, low toxicity and renewable character [1–5]. However, the low reaction kinetics of ethanol oxidation and the high fabrication cost limit the advancement of future energy technologies [6–8]. The electrocatalyst is a key factor in improving the velocities of ethanol oxidation and lowering the cost. Previous research results show that the performance of the ethanol oxidation could be significantly improved in alkaline media by using Pd as electrocatalyst [9–11]. Compared with Pt, Pd is a relatively abundant and less expensive resource [7,12]. Nevertheless, Pd is also a noble metal, so it is really necessary to increase the catalytic activities and reduce the loading of Pd electrocatalyst for commercial applications of DEFCs.

To achieve this goal, much research aimed at synthesizing different nanostructured Pd electrocatalysts and supporting them on various carbon materials [9,13–16]. Generally, the catalyst layer is prepared by painting or printing the suspension of catalyst and proton conducting ionomer (usually Nafion-H) onto the Nafion membrane and/or carbon electrode. However, Such structure provides poor mass transfer of reactant and large contact resistance at the interface between catalyst and electrode without considering the challenges in homogeneous dispersion of catalyst and reliable coating techniques [17]. To resolve these issues, a 3D electrode with opened-pore structure is desirable. The 3D interconnected porous structure of the electrode can increase the active sites and enhance the mass transfer of reactants or products, and thereby reduce the polarization and improve catalyst efficiency [18,19].

Nickel foam, a commercial material with extinguished electronic conductivity, low weight, and 3D cross-linked grid structure which allows providing high porosity and surface area, could be used as an ideal support of electrocatalysts [20]. The nickel foam would not only reduce the diffusion resistance of electrolyte but also enhance the facility of ion transportation and maintain the very smooth electron pathways in the rapid electrochemical reactions. Recently, nickel foam was investigated as a potential substrate for the cathode of alkaline fuel cells which showed enhanced performance [21]. Sun et al. reported that the nanostructured Ag and Pd-Ag electrodeposited on the nickel foam exhibited high catalytic activity and stable electrode performance for the reduction reaction of hydrogen peroxide [18,19]. The electrode provided a high surface area in the catalyst layer and offered lower mass transport resistance. In this paper, it is reported for the first time that hierarchically structured Pd electrocatalyst was directly electrodeposited on the nickel foam for ethanol electro-oxidation. The electroactivity

* Corresponding author. Fax: +86 931 8912582.
E-mail address: xucl@lzu.edu.cn (C.-L. Xu).

0378-7753/$ – see front matter © 2010 Elsevier B.V. All rights reserved.
doi:10.1016/j.jpowsour.2010.04.025

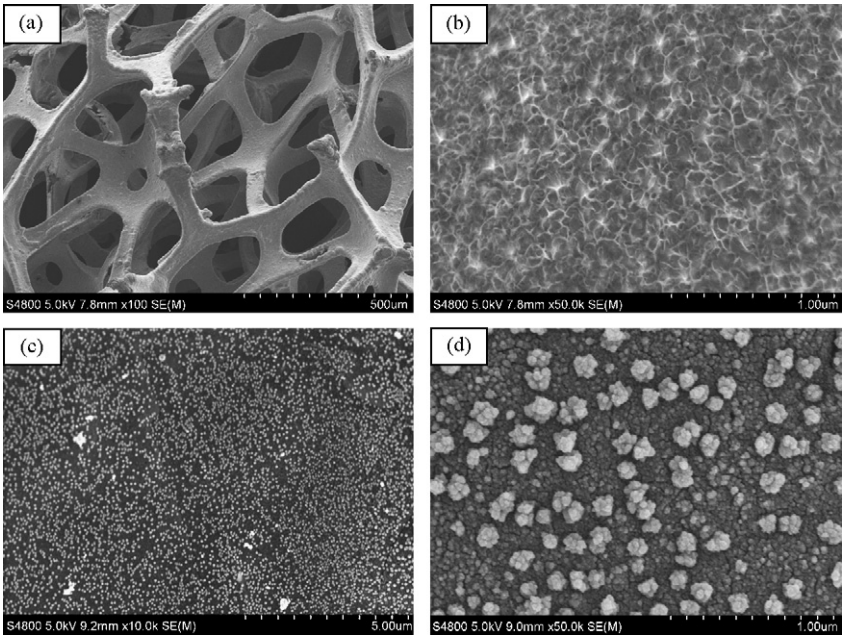

Fig. 1. FESEM micrographs of (a) an overview of nickel foam; (b) an enlarged view for the surface of nickel foam; (c) Pd coating deposited onto the surface of nickel foam; (d) an enlarged view of Pd coating.

towards the ethanol oxidation was evaluated by cyclic voltammetry. The results reveal that the 3D Pd/Nickel foam electrode possesses superior electrocatalytic activity and long-term stability, suggesting its potential application in DEFCs.

2. Experimental

2.1. Preparation of electrodes

Nickel foam (thickness: 1.8 mm, pore density: 110 ppi) was used as a support for the catalyst. Before the electrodeposition, nickel foam was rinsed with acetone and hydrochloric acid to clean and etch the metal surface. The electrodeposition was conducted by a CHI660b model Electrochemical Workstation (Chenhua, China) at a constant potential of −0.3 V with a three-electrode cell, which consisted of a saturated calomel electrode (SCE) as reference electrode, a 3.0 cm × 3.0 cm platinum plate as counter electrode and the treated nickel foam as the working electrode. The electrolyte was an aqueous solution containing 8.6 mM $PdCl_2$ and 0.49 M H_3BO_3. The deposition charge quantity was approximately 0.1454 C. The Pd loading was about 0.11 mg cm^{-2} estimated by Faraday's law. For comparison, the Pd film electrode with the same Pd loading was electrodeposited on the Ti substrate under the same condition.

2.2. Characterization of electrodes

The morphology of the electrodeposited Pd layer was characterized using field emission scanning electron microscope (FESEM, JEOL JSM-S4800). XRD data was collected using a Rigaku D/MAX 2400 diffractometer (Japan) with Cu Kα radiation (k = 1.5418 Å) operating at 40.0 kV, 60.0 mA. All electrochemical measurements were carried out in a conventional three-electrode cell on a CHI660b electrochemical workstation. The cell consisted of the as-prepared Pd/Nickel foam electrode as the working electrode, a Pt foil of 3.0 cm × 3.0 cm as the counter electrode, and Hg/HgO/1.0 M KOH (MMO) as reference electrode. Recent studies have demonstrated that the ethanol oxidation on a Pd electrode in alkaline media is significantly affected by the pH of the aqueous ethanol solution and the optimized KOH concentration is 1.0 M for the ethanol oxidation in terms of the peak current and peak potential [11,22]. Thus, in our study the concentration of KOH in the electrolyte is 1.0 M. The CV and stability experiments were performed in 1.0 M KOH aqueous solution in the absence or presence of 1.0 M ethanol at room temperature (23 ± 2 °C). The scan rate was 50 mV s^{-1} in the potential range of −0.8 to 0.2 V versus MMO. Prior to the experiments, the solution was deaerated with N_2 for 30 min.

3. Results and discussion

Fig. 1 shows the surface morphology and microstructure of the treated nickel foam and the as-prepared Pd/Nickel foam electrode. It can be seen that the nickel foam has 3D, porous and cross-linked grid structure (Fig. 1a). A close examination reveals that there are considerable uniform wrinkles on its surface (Fig. 1b). Fig. 1c displays the Pd coating deposited onto the surface of nickel foam. The surface of nickel foam is well covered by Pd particles. Interestingly, the Pd coating takes on hierarchical structure (Fig. 1d). Dense and uniform Pd nanoparticles with a size of ca. 10–40 nm are observed in the sublayer, while the superstructured layer is composed of many island-like Pd grains with size range from about 100 to 150 nm.

Fig. 2 shows the X-ray diffraction pattern of the as-prepared Pd/Nickel foam electrode. The peaks at 40.1°, 46.6°, and 68.1° can be assigned to (1 1 1), (2 0 0), and (2 2 0) crystalline plane diffraction peaks of face-centered cubic Pd metal (JCPDS No. 46-1043), respectively. In addition, nickel substrate shows the main characteristic peaks of face-centered cubic (JCPDS No. 04-0850) at 2θ = 44.5°, 51.8° and 76.4°, namely, the planes (1 1 1), (2 0 0) and (2 2 0). The results further confirm that Pd electrocatalyst are successfully electrodeposited on the nickel foam.

The CVs of the Pd/Nickel foam electrode (curves a, Pd loading: 0.11 mg cm^{-2}), the Pd film electrode (curves b, Pd loading: 0.11 mg cm^{-2}) and the nickel foam electrode (curves c) in 1 M KOH without ethanol solution are presented in Fig. 3. As is well known, the charge for the underpotential deposition (UPD) of hydrogen is required to calculate the electrochemical active surface (EAS). The charge is 210 μC cm^{-2} for Pt [23], while the charge for Pd cannot be accurately obtained owing to the interference of hydrogen absorp-

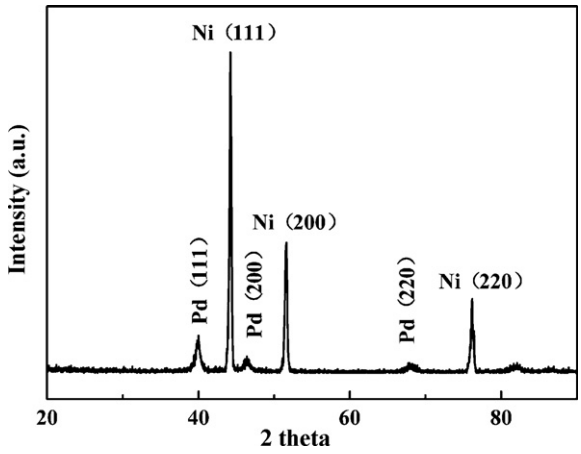

Fig. 2. XRD pattern of Pd/Nickel foam electrode.

tion in Pd [24,25]. According to the previous literatures [26,27], the coulombic charge for the reduction of palladium oxide can be employed to calculate the EAS of the electrodes. From Fig. 3, it is obvious that the area of palladium oxide reduction in the potential range $-0.5\,V < E < 0\,V$ on the Pd/Nickel foam electrode is much larger than that of Pd film electrode. This demonstrates that the Pd/Nickel foam electrode has higher electrochemical active surface, most likely due to the 3D, porous and cross-linked grid structure of nickel foam, well-dispersion and hierarchical structure of Pd electrocatalyst on the nickel foam, which provide the increased active sites and the enhanced mass diffusion.

The electrocatalytic activity of the above electrodes towards ethanol oxidation was investigated by CV in 1.0 M C_2H_5OH + 1.0 M KOH aqueous solution. The typical curves are shown in Fig. 4 (the inset is enlarged view). It exhibits that no current peak appears for ethanol oxidation on the nickel foam electrode (curve c), indicating that the nickel foam electrode has no electrocatalytic activity for ethanol oxidation in the potential range. As is seen from curve a and curve b in Fig. 4, the electro-oxidation of ethanol is characterized by two well-defined current peaks in the forward and reverse scans, associated with the oxidation of freshly chemisorbed species coming from ethanol adsorption and removal of carbonaceous species not completely oxidized in the forward scan, respectively [26]. In the forward scan, the oxidation peak current densities are 107.7 and 13.2 mA cm^{-2} on the Pd/Nickel foam and Pd film electrode, respectively. The anodic peak current density of the Pd/Nickel foam

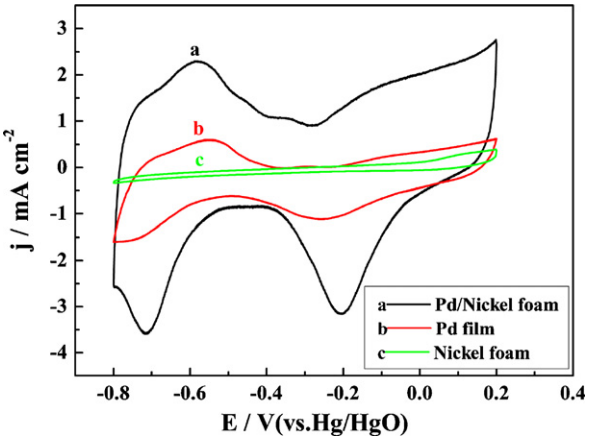

Fig. 3. CV curves of the different electrodes in 1 M KOH at a scan rate of 50 mV s^{-1}: (a) Pd/Nickel foam electrode (Pd loading: 0.11 mg cm^{-2}); (b) Pd film electrode (Pd loading: 0.11 mg cm^{-2}); (c) nickel foam.

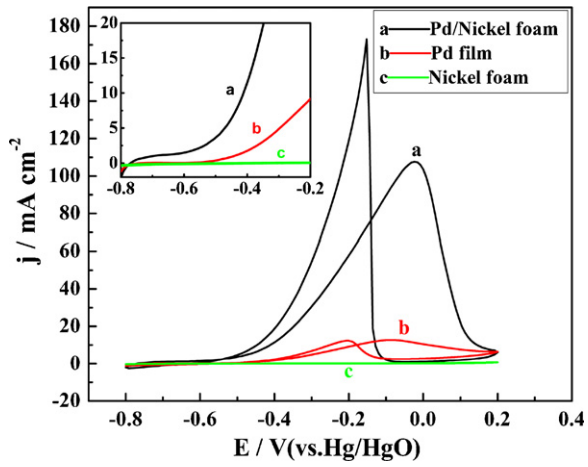

Fig. 4. CV curves of the different electrodes in 1 M KOH + 1 M C_2H_5OH at a scan rate of 50 mV s^{-1}: (a) Pd/Nickel foam electrode (Pd loading: 0.11 mg cm^{-2}); (b) Pd film electrode (Pd loading: 0.11 mg cm^{-2}); (c) nickel foam (inset: enlarged view).

electrode is above 8 times than that of Pd film, which is consistent with the conclusion of EAS test. In addition, compared with some reported Pd electrocatalysts and the commercial Pt-Ru/C electrocatalyst with higher catalyst loading, the Pd/Nickel foam electrode presents much higher peak current density for ethanol oxidation under the same test condition [8–10,13,14,26,28,29]. From the inset in Fig. 4, the onset potential for ethanol oxidation on Pd film is about −0.54 V. By contrast, the onset potential for ethanol electro-oxidation on Pd/Nickel foam electrode is −0.63 V, which is 90 mV more negative than that of Pd film electrode. This suggests that the Pd/Nickel foam electrode is able to significantly improve the kinetics of the ethanol oxidation reaction. The Pd/Nickel foam electrode shows a remarkably enhanced performance towards ethanol oxidation in alkaline medium in comparison with the Pd film electrode in terms of anodic peak current density and onset potential.

The long-term stability of Pd/Nickel foam electrode and Pd film electrode are also carried out by CV and the corresponding results are given in Fig. 5. It is noted that the peak current density of the Pd/Nickel foam electrode increases with increasing cycle number within the first 200 cycles due to the fact that the electrolyte needs a process to fully penetrate into the Pd coating. At the 200th cycle, the peak current density of the sample reaches an extremely high value of 107.7 mA cm^{-2}. Subsequently, it decreases gradually with successive scans and finally remains 98.1% of the maximum value. While for the Pd film, the peak current density only remains 14.2% of

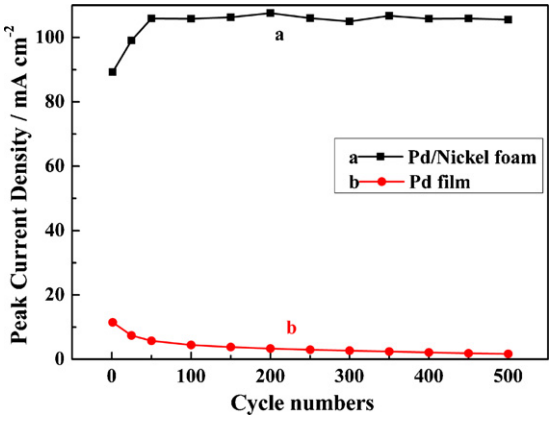

Fig. 5. Long-term stability of Pd/Nickel foam (a) and Pd film electrode (b) in 1 M KOH + 1 M C_2H_5OH at a scan rate of 50 mV s^{-1}.

its initial value after a monotone decrease in 500 cycles. The results demonstrate that the Pd/Nickel foam electrode possesses more excellent stability than the Pd film electrode. The loss of catalytic activity can be explained in terms of poisoning mechanism of the intermediate species during the ethanol oxidation reaction on the Pd electrodes. It also may be due to the structure change of the Pd nanoparticles during repeated potential cycling [30]. However, the novel structure of the Pd/Nickel foam electrode not only enhances the mass transfer of reactants or products but also reduces the reaction resistance, which probably helps to stabilize the structure of Pd electrocatalyst and benefits for the removing of poisoning species.

4. Conclusions

A 3D hierarchically structured Pd electrode has been successfully fabricated by directly electrodepositing Pd nanoparticles on the nickel foam. The well-dispersion and hierarchical structures of Pd nanoparticles on the nickel foam provide a much larger surface area for reaction, leading to the effective utilization of the electrode material. The Pd/Nickel foam electrode displays improved electrocatalytic activity and stability for ethanol oxidation. As a result, the Pd/Nickel foam electrode with superb performance, relatively low cost as well as simple fabrication procedure is a promising candidate for the conventional carbon supported electrode for the wide applications in DEFCs.

Acknowledgements

This work was supported by grants from the Natural Science Foundation of China (NNSFC NO.20903050), the Fundamental Research Funds for the Central University (Lzujbky-2009-28), the China Postdoctoral Science Foundation (20070420133), Interdisciplinary Innovation Research Fund for Young Scholars, Lanzhou University and Fund of Xinjiang Uygur Autonomous Region University young Youth Scholars (XJEDU2008S46).

References

[1] S. Rousseau, C. Coutanceau, C. Lamy, J.-M. Léger, J. Power Sources 158 (2006) 18–24.
[2] H. Wang, Z. Jusys, R.J. Behm, J. Phys. Chem. B 108 (2004) 19413–19424.
[3] S.Q. Song, P. Tsiakaras, Appl. Catal. B-Environ. 63 (2006) 187–193.
[4] C. Lamy, A. Lima, V. LeRhun, F. Delime, C. Coutanceau, J.-M. Léger, J. Power Sources 105 (2002) 283–296.
[5] Z.-B. Wang, G.-P. Yin, J. Zhang, Y.-C. Sun, P.-F. Shi, J. Power Sources 160 (2006) 37–43.
[6] X.Y. Zhang, W. Lu, J.Y. Da, H.T. Wang, D.Y. Zhao, P. Webley, Chem. Commun. 2009 (2009) 195–197.
[7] C. Bianchini, P.K. Shen, Chem. Rev. 109 (2009) 4183–4206.
[8] Y. Wang, T. Nguyen, C. Wang, X. Wang, Dalton Trans. (2009) (2009) 7606–7609.
[9] C.W. Xu, P.K. Shen, Y.L. Liu, J. Power Sources 164 (2007) 527–531.
[10] C.W. Xu, H. Wang, P.K. Shen, S.P. Jiang, Adv. Mater. 19 (2007) 4256–4259.
[11] G.F. Cui, S.Q. Song, P.K. Shen, A. Kowal, C. Bianchini, J. Phys. Chem. C 113 (2009) 15639–15642.
[12] Platinum Met. Rev. 53 (2009) 48–49, http://www.platinummetalsreview.com/dynamic/article/view/53-1-48-49.
[13] L.D. Zhu, T.S. Zhao, J.B. Xu, Z.X. Liang, J. Power Sources 187 (2009) 80–84.
[14] D.B. Chu, J. Wang, S.X. Wang, L.W. Zha, J.G. He, Y.Y. Hou, Y.X. Yan, H.S. Lin, Z.W. Tian, Catal. Commun. 10 (2009) 955–958.
[15] C.W. Xu, Z.Q. Tian, P.K. Shen, S.P. Jiang, Electrochim. Acta 53 (2008) 2610–2618.
[16] F.P. Hu, Z.Y. Wang, Y.L. Li, C.M. Li, X. Zhang, P.K. Shen, J. Power Sources 177 (2008) 61–66.
[17] R. Chetty, K. Scott, Electrochim. Acta 52 (2007) 4073.
[18] W.Q. Yang, S.H. Yang, W. Sun, G.Q. Sun, Q. Xin, Electrochim. Acta 52 (2006) 9–14.
[19] W.Q. Yang, S.H. Yang, W. Sun, G.Q. Sun, Q. Xin, J. Power Sources 160 (2006) 1420–1424.
[20] G.W. Yang, C.L. Xu, H.L. Li, Chem. Commun. (2008) 6537–6539.
[21] F. Bidault, D.J.L. Brett, P.H. Middleton, N. Abson, N.P. Brandon, Int. J. Hydrogen Energy 34 (2009) 6799–6808.
[22] Z.X. Liang, T.S. Zhao, J.B. Xu, L.D. Zhu, Electrochim. Acta 54 (2009) 2203–2208.
[23] A. Pozio, M. De Francesco, A. Cemmi, F. Cardellini, L. Giorgi, J. Power Sources 105 (2002) 13–19.
[24] L. Xiao, L. Zhuang, Y. Liu, J.T. Lu, H.D. Abruña, J. Am. Chem. Soc. 131 (2009) 602–608.
[25] M. Łukaszewski, M. Grdeń, A. Czerwiński, J. Solid State Electrochem. 9 (2005) 1–9.
[26] R.N. Singh, A. Singh, Anindita, Carbon 47 (2009) 271–278.
[27] S.T. Nguyen, H.M. Law, H.T. Nguyen, N. Kristian, S.Y. Wang, S.H. Chan, X. Wang, Appl. Catal. B-Environ. 91 (2009) 507–515.
[28] J. Bagchi, S.K. Bhattacharya, J. Power Sources 163 (2007) 661–670.
[29] J. Bagchi, S.K. Bhattacharya, Transition Met. Chem. 33 (2008) 113–120.
[30] D.-J. Guo, H.-L. Li, Electroanalysis 17 (2005) 869–872.